Model Predictive Control Based Demand Response Scheme for Peak Demand Reduction in a Smart Campus Integrated Microgrid

YASMINE ACHOUR[1], AHMED OUAMMI[2], AND DRISS ZEJLI[1]

[1]Advanced Systems Engineering Laboratory, Ibn Tofail University, Kenitra 14000, Morocco
[2]Centre for Sustainable Development, College of Arts and Sciences, Qatar University, Doha, Qatar

Corresponding author: Ahmed Ouammi (aouammi@qu.edu.qa)

ABSTRACT This paper presents an effective solution to manage the power flows exchanges in a campus integrated microgrid for peak reduction/shaving purposes. The campus integrated microgrid is composed of photovoltaic parking shades, an energy storage system, electric vehicles and bikes, loads, an advanced metering infrastructure, and a smart control unit. The latter is based on Model Predictive Control (MPC) whose objective is to reduce/shave the peak load of the campus while satisfying the Energy Storage System ESS, electrical Vehicles (EVs) and Electrical Bikes (EBs) state of charge. The proposed strategy aims to take the advantage of combining storage and photovoltaic (PV) systems to Vehicle to Campus (V2C) and Bike to Campus (B2C) concepts to support the microgrid to pay the minimum billing power while ensuring a good service quality to the EVs and EBs users. For that, the integration of the renewable energy sources and the different storage systems into the microgrid is modeled, and the MPC-based optimization framework is formulated. Besides, the results related to the application of the MPC to real case studies are presented, integrating the effects of static and dynamic weighting factors on the microgrid operation.

INDEX TERMS Campus integrated microgrid, model predictive control, demand response, peak reduction, electric vehicles, electric bikes, renewable energy.

I. NOMENCLATURE

A. ACRONYMS

MPC	Model Predictive Control.
DSM	Demand Side Management.
DNO	Distributed Network Operator.
PV	Photovoltaic.
DR	Demand Response.
EV	Electric Vehicle.
EB	Electric Bike.
V2C	Vehicle to Campus.
B2C	Bike to Campus.
CMS	Campus Management System.
ESS	Energy Storage System.
RES	Renewable Energy Sources.
RMSE	Root Mean Square Error.

B. PARAMETERS

Δt	Time interval [h]	1.
I_{sc}	PV module short circuit current [A]	9.98.
I_{mp}	PV module maximum power current [A]	9.5.
V_{mp}	PV module maximum power voltage [V]	33.16.
V_{oc}	PV module open circuit voltage [V]	40.53.
I_{st}	Standard light intensity	1000.
μ	PV module voltage temperature coefficient [V/°C] -0.3.	
γ	PV module current temperature coefficient [A/°C] 0.06.	
$\eta_{pv,s}$	Serial connection number of PV modules	156.
$\eta_{pv,p}$	Parallel connection number of PV module strings 1.	
η_{loss}	PV connection loss	0.9.
$\eta_{char}^{ev,i}$	The ith EV charging efficiency	0.9.
$\eta_{dis}^{ev,i}$	The ith EV discharging efficiency	0.9.
$\eta_{char}^{eb,i}$	The ith EB charging efficiency	0.9.
$\eta_{dis}^{eb,i}$	The ith EB discharging efficiency	0.9.

η_{char}^{ess}	ESS charging efficiency 0.9.
η_{dis}^{ess}	ESS discharging efficiency 0.9.
$u_{pv,min}$	PV power output lower bound [kW] 0.
$u_{pv,max}$	PV power output upper bound [kW] 49.14.
$u_{ess,min}$	ESS state of charge lower bound [kWh] 10.
$u_{ess,max}$	ESS state of charge upper bound [kWh] 96.
u_{lim}	Subscribed power limit [kW] 100.
$u_{ev,min}(i,t)$	The ith EV state of charge lower bound [kWh] 1.45.
$u_{ev,max}(i,t)$	The ith EV state of charge upper bound [kWh] 14.5.
$u_{eb,min}(i,t)$	The ith EB state of charge lower bound [kWh] 0.046.
$u_{eb,max}(i,t)$	The ith EB state of charge upper bound [kWh] 0.468.
$u_{char,min}^{ev}(i,t)$	The ith EV minimum charging rate [kW] 0.
$u_{char,max}^{ev}(i,t)$	The ith EV maximum charging rate [kW] 3.7.
$u_{dis,min}^{ev}(i,t)$	The ith EV minimum discharging rate [kW] 0.
$u_{dis,max}^{ev}(i,t)$	The ith EV maximum discharging rate [kW] 3.7.
$u_{char,min}^{eb}(i,t)$	The ith EB minimum charging rate [kW] 0.
$u_{char,max}^{eb}(i,t)$	The ith EB maximum charging rate [kW] 0.1.
$u_{dis,min}^{eb}(i,t)$	The ith EB minimum discharging rate [kW] 0.
$u_{dis,max}^{eb}(i,t)$	The ith EB maximum discharging rate [kW] 0.1.
$u_{char,min}^{ess}$	ESS minimum charging rate [kW] 0.
$u_{char,max}^{ess}$	ESS maximum charging rate [kW] 4.
$u_{dis,min}^{ess}$	ESS minimum discharging rate [kW] 0.
$u_{dis,max}^{ess}$	ESS maximum discharging rate [kW] 6.85.
$\bar{u}_{campus}$	Dynamic reference of the campus loads [kW] See Results section.
$\bar{u}_{ev}(i,t)$	Desired stored energy state in the ith EV [kWh] See Results section.
$\bar{u}_{eb}(i,t)$	Desired stored energy state in the ith EB [kWh] See Results section.
$\bar{u}_{ess}$	Desired stored energy state in the battery [kWh] 96.

C. VARIABLES

$u_{char}^{ev}(i,t)$	The ith EV charging power [kW].
$u_{dis}^{ev}(i,t)$	The ith EV discharging power [kW].
$u_{char}^{eb}(i,t)$	The ith EB charging power [kW].
$u_{dis}^{eb}(i,t)$	The ith EB discharging power [kW].
$t_{i,av}$	The ith EV arrival time.
$t_{i,dv}$	The ith EV departure time.

$\sigma_{i,av}$	The ith EV standard deviation of the arrival time.
$\sigma_{i,dv}$	The ith EV standard deviation of the departure time.
$\mu_{i,av}$	The ith EV distribution mean of the arrival time.
$\mu_{i,dv}$	The ith EV distribution mean of the departure time.
$t_{i,ab}$	The ith EB arrival time.
$t_{i,db}$	The ith EB departure time.
$\sigma_{i,ab}$	The ith EB standard deviation of the arrival time.
$\sigma_{i,db}$	The ith EB standard deviation of the departure time.
$\mu_{i,ab}$	The ith EB distribution mean of the arrival time.
$\mu_{i,db}$	The ith EB distribution mean of the departure time.
u_{char}^{ess}	ESS charging power [kW].
u_{dis}^{ess}	ESS discharging power [kW].
χ	Campus load weighting factor.
ψ	EV weighting factor.
λ	EB weighting factor.
θ	ESS weighting factor.
u_{pv}	PV power [kW].
u_{ev}	EV state of charge [kWh].
u_{eb}	EB state of charge [kWh].
u_{ess}	ESS state of charge [kWh].
u_{campus}	Campus total power loads [kW].
$u_{pv,ess}$	Power charged to ESS coming from PV [kW].
$u_{pv,dno}$	Power sold to DNO coming from PV [kW].
$u_{pv,campus}$	Power sent from PV to satisfy the campus loads.
$u_{pv,ev}(i,t)$	Power charged to the ith EV coming from PV [kW].
$u_{pv,eb}(i,t)$	Power charged to the ith EB coming from PV [kW].
$u_{ess,campus}$	Power discharged from ESS to satisfy the campus loads [kW].
$u_{dno,campus}$	Power sent from DNO to satisfy the campus loads [kW].
$u_{ev_{dis},campus}(i,t)$	Power discharged from the ith EV to satisfy the campus loads [kW].
$u_{eb_{dis},campus}(i,t)$	Power discharged from the ith EB to satisfy the campus loads [kW].
$u_{ess,ev}$	Power charged to EV coming from ESS [kW].
$u_{ess,eb}$	Power charged to EB coming from ESS [kW].

II. INTRODUCTION

Recently, peak load has increased at a rapid rate due to changing demographics and economic growth. Peak load is defined as the periods when electricity consumption becomes

very high and can occur in daily, monthly, seasonal or annual cycles. Its continuous increase over the next few years maximizes the chances of microgrids breakdowns, elevates the possibilities of their stability and sustainability reduction, and increases the marginal cost of supply [1]. Thus, peak load control becomes a major concern of utilities and a promising area of research. It is a process that consists of smoothing the load curve by reducing the electrical power consumption and shifting it to times of lower load [2]. Therefore, it offers interesting benefits for the utility provider such as improving the reliability and power quality [3], avoiding voltage fluctuations and devastating blackouts, and it also reaps financial benefits to end users by shifting the peak load to periods of low cost electricity [4].

Peak load reduction/shaving can be done using a variety of methods and techniques. The two most used strategies are the integration of external storage and the demand side management (DSM) [5]. The first strategy consists of implementing backup suppliers such as energy storage systems (ESS) and electric vehicles (EVs). These storage-based peak load shaving systems can be used in residential and commercial buildings, institutional campuses, industries, and grids. They provide economic benefits as they act as an additional independent energy source during peak demand and thus attenuate the need to use high-priced electricity generation. Therefore, many studies aiming to reduce the peak demand with the help of ESS have been developed [6], [7] [8]. More others concerning the ESS optimal sizing that minimizes the operating cost of the microgrid have been proposed [9], [10]. Also, others regarding the use of EVs batteries for peak shaving purposes have been considered [11]–[13].

However, the second strategy remains the most potential for peak shaving. DSM encourages to adjust power consumption to significantly reduce energy waste, peak load demand, and monetary cost of energy [14]. It is structured in two strategies: energy efficiency and demand response (DR). Energy efficiency tends to facilitate minimal energy consumption [5], while DR modifies the pattern of usual consumption in response to price fluctuations [15]. DR programs offer a significant amount of price reduction to the end users [16]. It is an important peak shaving strategy that should be part of the system operations in the future network [17]. An example of DR-based peak shaving has been proposed for a home-to-grid system and has achieved good results in terms of cost reduction through load shifting [18]. It has been also applied in the agricultural sector to reduce the peak demand of responsive farms [19]. More, various studies aiming to achieve maximum peak shaving through DR have been developed using different algorithms [20]–[22]. In this context, special attention was paid to model predictive control, where its application to an existing grid connected household with PV battery allowed to reduce peaks in PV energy and load demands [23]. This strategy has also been designed to maximize the use of battery by prioritizing the load demand for a single electricity price scenario [24]. It has allowed annual energy savings of 13.5% as well, when it was used to find

the optimal schedule of battery avoiding unnecessary peak reduction [25]. On the whole, the use of DR algorithms has become popular under the smart microgrid paradigm, especially with the integration of bidirectional communication capabilities that enabled utilities to collect/provide real time information from/to consumers. DR has activated the change of microgrid status to an active contributor that enable end users to participate actively in managing their consumptions. Its main aim is to support power systems to increase energy security and reliability [26].

In this paper, an innovative DR scheme for peak load reduction in an institutional campus integrated microgrid including PV systems, ESS, EBs and EVs is developed. The proposed strategy is based on model predictive control and can be implemented as a supervisory real-time control in the utility systems to effectively manage the microgrid power flows while coping with renewable energy sources uncertainties and while satisfying the complicated operating constraints. The microgrid is used to equilibrize the fluctuations of the campus load and to achieve energy balances in a way to import its energy needs from the DNO when the demand is below the subscribed power, and in the opposite case, the CMS will be responsible to dispatch the available microgrid local energy according to the MPC-based strategy. All in all, the contributions of this paper can be summarized in developing a practical control framework expressed as a constrained optimization problem embedded in a model predictive control scheme to optimally control the operation of a campus integrated microgrid to shave/reduce peak load in case of occurrence, optimize the ESS state of charge and ensure the EVs and EBs desired departure state of charge. The developed predictive algorithm could represent an attractive field for engineers and researchers. The power flows control in a campus integrated microgrid is introduced to improve the satisfaction of the quality of service, here defined as the reduction of peak loads and the EVs/ EBs charging preferences. In the proposed framework, the microgrid is used to reduce the peak load, and to compensate the variabilities of the campus's load and well as decreasing its energy bill. Especially, when the power load is under an agreed bilateral power limit, the campus purchases its requirements from the electric grid; while when the power load is over this fixed power limit, the energy management system is responsible of generating the optimal control of power flows at the microgrid level to fulfill as possible the peak load. To test the MPC strategy through several case studies, where the effects of different priorities on the tracking references and on the optimal solution is analyzed via numerical results. The case studies are adopted and discussed to demonstrate the benefits and feasibility of the proposed optimization approach.

The rest of this paper is organized as follows. In Section II, the campus integrated microgrid architecture and mathematical modeling is presented. In Section III, the MPC-based optimal operation if formulated. In Section IV, the performance of the proposed scheme is demonstrated through a concrete case study. And finally, a brief conclusion is given in Section V.

III. MICROGRID MODELING

A. MICROGRID ARCHITECTURE

The campus microgrid consists of several institutional buildings electrically connected to the DNO through the campus network, and equipped with a local energy production, a storage system, and a smart management system. As it can be seen in Fig. 1, the university campus microgrid integrates several units: 1) A set of photovoltaic modules forming car parking shades; 2) An ESS improving the stability and the reliability of the supply; 3) Electric vehicles and bikes improving the microgrid energy dispatch flexibility; 4) Loads representing the campus buildings; and 5) A CMS responsible for delivering the optimal power control strategy.
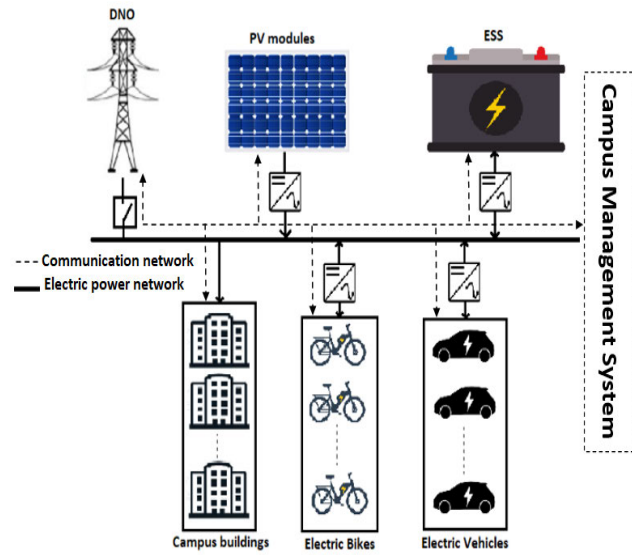
FIGURE 1. Microgrid architecture.

In fact, the CMS is in charge to control the operation of the university campus microgrid to mitigate the peak load demand. Its communication infrastructure relies on centralized communication where a single MPC-based main controller collects the required data from the different microgrid components and performs the necessary actions. The CMS ensures the electric supply of the campus buildings directly from the DNO following an established bilateral contract with the electricity supplier and on the basis of invoicing according to the consumption brackets. However, if the campus load exceeds the power subscribed, the CMS should efficiently harness the different microgrid energy sources to reduce the peak, namely: the energy produced by the PV and the energy stored in ESS, EV and EB. The microgrid PV generators are used mainly to meet the varying loads of EV and EB, and the surplus generated should be routed to ESS and/or exchanged with the DNO after satisfying the campus load in peak periods, following an optimal control strategy implemented in the CMS.

B. PHOTOVOLTAIC PARKING SHADES MODELING

Photovoltaic production depends mainly on the solar radiation of the site on which the panels are installed, in addition to the technical characteristics of the panel itself. The optimum voltage V_{pv} and current I_{pv} generated are [27]:

$$I_{pv}(t) = I_{sc}\left\{1 - \alpha\left[exp\left(\frac{V_{mp}}{\beta V_{oc}}\right) - 1\right]\right\} + \Delta I(t) \quad (1)$$

$$V_{pv}(t) = V_{mp}\left[1 + 0.0539log\left(\frac{I(t)}{I_{st}}\right)\right] + \mu\Delta T(t) \quad (2)$$

where,

$$\alpha = \left(1 - \frac{I_{mp}}{I_{sc}}\right)exp\left[-\frac{V_{mp}}{\beta V_{oc}}\right] \quad (3)$$

$$\beta = \frac{\frac{V_{mp}}{V_{oc}} - 1}{ln\left(1 - \frac{I_{mp}}{I_{sc}}\right)} \quad (4)$$

$$\Delta I(t) = \gamma\left(\frac{I(t)}{I_{st}}\right)\Delta T(t) + \left(\frac{I(t)}{I_{st}} - 1\right)I_{sc} \quad (5)$$

$$\Delta T(t) = T_{amb} + 0.02I(t) \quad (6)$$

The PV power generation is

$$u_{pv}(t) = \eta_{pv,s}\eta_{pv,p}V_{pv}(t)I_{pv}(t)\eta_{loss} \quad (7)$$

C. ELECTRIC VEHICLES MODELING

The evolution of the energy stored in the electric vehicles available in the microgrid can be expressed as follows [20] [28]:

$$u_{ev}(i, t+\Delta t) = u_{ev}(i, t) + \eta_{char}^{ev,i}u_{char}^{ev}(i, t)\Delta t \\ -\eta_{dis}^{ev,i}u_{dis}^{ev}(i, t)\Delta t \quad (8)$$

where $t \in [t_{i,av}\ t_{i,dv}]$ is the scheduling time horizon, $t_{i,av}$ and $t_{i,dv}$ are respectively, the arrival and departure time vectors of the ith EV available in the campus. They are modeled using the Gaussian distributions as follows:

$$t_{i,av}(x) = \frac{1}{\sigma_{i,av}\sqrt{2\pi}}exp^{\left(-\frac{(x-\mu_{i,av})^2}{2\sigma_{i,av}^2}\right)} \quad (9)$$

$$t_{i,dv}(x) = \frac{1}{\sigma_{i,dv}\sqrt{2\pi}}exp^{\left(-\frac{(x-\mu_{i,dv})^2}{2\sigma_{i,dv}^2}\right)} \quad (10)$$

D. ELECTRIC BIKES MODELING

The evolution of the energy stored in the electric bikes available in the microgrid can be expressed as follows [20] [28]:

$$u_{eb}(j, t+\Delta t) = u_{eb}(j, t) + \eta_{char}^{eb,j}u_{char}^{eb}(j, t)\Delta t \\ -\eta_{dis}^{eb,j}u_{dis}^{eb}(j, t)\Delta t \quad (11)$$

where $t \in [t_{j,ab}\ t_{j,db}]$ is the scheduling time horizon, $t_{j,ab}$ and $t_{j,db}$ are respectively, the arrival and departure time vectors of the ith EB available in the campus. They are modeled using the Gaussian distributions as follows:

$$t_{j,ab}(x) = \frac{1}{\sigma_{j,ab}\sqrt{2\pi}}exp^{\left(-\frac{(x-\mu_{j,ab})^2}{2\sigma_{j,ab}^2}\right)} \quad (12)$$

$$t_{j,db}(x) = \frac{1}{\sigma_{j,db}\sqrt{2\pi}}exp^{\left(-\frac{(x-\mu_{j,db})^2}{2\sigma_{j,db}^2}\right)} \quad (13)$$

E. ENERGY STORAGE SYSTEM

The energy storage system dynamics is expressed as [29]:

$$u_{ess}(t+\Delta t) = u_{ess}(t) + \eta_{char}^{ess} u_{char}^{ess}(t)\,\Delta t - \eta_{dis}^{ess} u_{dis}^{ess}(t)\,\Delta t \tag{14}$$

IV. MPC-BASED OPTIMAL OPERATION FORMULATION
A. DEMAND RESPONSE STRATEGY

In Morocco, university campuses are subject to electricity tariffs which vary according to consumption brackets. Generally, the tariff option consists of a kWh price which fluctuates according to the exceeding of the subscribed power set at 100 kW, from which the price per kWh becomes higher [30]. For this, and in order to minimize energy bills, a demand response consisting of implementing the microgrid load management strategy is proposed to change the campus power consumption profile during price peaks. This strategy is implemented in the CMS and is based on the MPC in order to optimally provide the peak load of the campus. Its objective is to keep the power demand of the electrical network below the subscribed power, through the proper exploitation of the energy produced locally and the energy stored in the ESS, EV and EB.

B. MPC-BASED OPERATION SCHEDULING

The MPC strategy relies on dynamic models and available measurements to predict the future behavior of a process, and thus calculate its optimal control sequence. This involves optimizing an objective function over a control horizon (Nc) submitted to the process model, with respect to future predictions, while coping with constraints on inputs and outputs. In fact, at each time t, the predictions of the controlled variables are computed up to a time horizon (Np), to determine the future control sequence for each power flow of the microgrid. However, only the first step of the calculated control law is implemented at the next clock stroke. All these steps are then repeated according to the receding horizon principle, allowing to compute the new control sequence. The main advantage of MPC is the fact that it allows to optimize the current time interval, while considering future intervals. In addition, its main strength is its ability to handle multiple inputs and outputs, as well as equal and inequal constraints.

The MPC basic structure block diagram is depicted in Fig. 2:

In this study, the main idea is to optimally manage the microgrid power flows in a way to reduce the peak load, by repeatedly solving online an optimal control problem, aiming to minimize the objective function delivered by the main controller, subject to constraints on the manipulated parameters.

C. OPTIMIZATION PROBLEM FORMULATION
1) OBJECTIVE FUNCTION

In this paper, the objective function is composed of 4 sub-objective ones. The first one is associated with satisfying
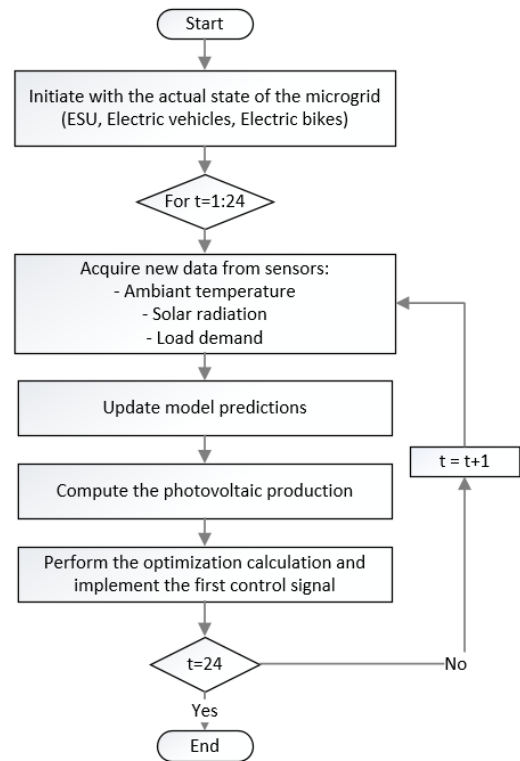

FIGURE 2. Model predictive control scheme.

the university campus loads. In fact, the CMS decides on the amount of energy to be purchased from the DNO and on the amount of energy to be drawn from the microgrid so as to avoid exceeding the peak load. In other words, the CMS aims to shave/reduce the campus peak load in period of high demands taking advantages of the storage and of the V2C and B2C concepts. The second and third ones are related to ensure the desired departure state of the EV and EB defined by their users. However, in order to ensure an adequate level of energy security for their recharge in the event of a PV energy shortage, the fourth term envisages maximizing the energy level of the ESS to its optimal working level.

The objective function minimizes the dual costs of quadratic terms defined as follows:

$$J = \chi \sum_{t=1}^{T} (u_{campus}(t+k) - \overline{u_{campus}(t+k)})^2$$
$$+ \psi \sum_{t=1}^{T}\sum_{i=1}^{I} (u_{ev}(i,t+k) - \overline{u_{ev}(i,t+k)})^2$$
$$+ \lambda \sum_{t=1}^{T}\sum_{j=1}^{J} (u_{eb}(j,t+k) - \overline{u_{eb}(j,t+k)})^2$$
$$+ \theta \sum_{t=1}^{T} (u_{ess}(t+k) - \overline{u_{ess}(t+k)})^2 \tag{15}$$

2) STATE EQUATIONS

The power generated by the solar parking shades is:

$$u_{pv}(t) = u_{pv,ess}(t) + u_{pv,dno}(t) + u_{pv,campus}(t)$$
$$+ \sum_{1}^{I} u_{pv,ev}(i,t) + \sum_{1}^{J} u_{pv,eb}(j,t) \quad (16)$$

The power balance is as follows:

$$u_{campus}(t) = u_{ess,campus}(t) + u_{dno,campus}(t) + u_{pv,campus}(t)$$
$$+ \sum_{i=s\geq1}^{S\leq I} u_{ev_{dis},campus}(i,t) + \sum_{j=l\geq1}^{L\leq J} u_{eb_{dis},campus}(i,t)$$
$$(17)$$

The power used to charge the electric bikes and vehicles is supplied by the solar parking shades and/or the energy storage system:

$$u_{char}^{ev}(i,t) = u_{pv,ev}(i,t) + u_{ess,ev}(i,t) \quad (18)$$
$$u_{char}^{eb}(j,t) = u_{pv,eb}(j,t) + u_{ess,eb}(j,t) \quad (19)$$

The power discharged from the energy storage system is:

$$u_{dis}^{ess}(t) = u_{ess,campus}(t) + \sum_{1}^{I} u_{ess,ev}(i,t) + \sum_{1}^{J} u_{ess,eb}(j,t)$$
$$(20)$$

The power discharged from the electrical vehicles and bikes and not dedicated to their operation is sent to the local grid:

$$u_{dis}^{ev}(i,t) = u_{ev,r}(j,t) + u_{ev_{dis},campus}(i,t) \quad (21)$$
$$u_{dis}^{eb}(j,t) = u_{eb,r}(j,t) + u_{eb_{dis},campus}(j,t) \quad (22)$$

3) CONSTRAINTS

The photovoltaic power generation is constrained between an upper and lower bound:

$$u_{pv,min}(t) < u_{pv}(t) < u_{pv,max}(t) \quad (23)$$

The stored energy has also upper and lower bounds:

$$u_{ess,min}(t) < u_{ess}(t) < u_{ess,max}(t) \quad (24)$$

The contribution of the PV modules, in addition to the energy storage system and the electric vehicles and bikes batteries to supply the campus load is set equal to zero below the subscribed power limit:

$$u_{pv,campus}(t) = 0 \ if \ u_{campus}(t) < u_{lim} \quad (25)$$
$$u_{ess,campus}(t) = 0 \ if \ u_{campus}(t) < u_{lim} \quad (26)$$
$$u_{ev\_dis,campus}(j,t) = 0 \ if \ u_{campus}(t) < u_{lim} \quad (27)$$
$$u_{eb\_dis,campus}(j,t) = 0 \ if \ u_{campus}(t) < u_{lim} \quad (28)$$

The energy stored in each electric bike's and vehicle's batteries should satisfy the capacity limits:

$$u_{ev,min}(i,t) < u_{ev}(i,t) < u_{ev,max}(i,t) \quad (29)$$
$$u_{eb,min}(j,t) < u_{eb}(i,t) < u_{eb,max}(j,t) \quad (30)$$

The charging and discharging rates of the energy storage system and the electric vehicles and bikes have upper and lower bounds:

$$u_{char,min}^{ev}(i,t) < u_{char}^{ev}(i,t) < u_{char,max}^{ev}(i,t) \quad (31)$$
$$u_{dis,min}^{ev}(i,t) < u_{dis}^{ev}(i,t) < u_{dis,max}^{ev}(i,t) \quad (32)$$
$$u_{char,min}^{eb}(j,t) < u_{char}^{eb}(j,t) < u_{char,max}^{eb}(j,t) \quad (33)$$
$$u_{dis,min}^{eb}(j,t) < u_{dis}^{eb}(j,t) < u_{dis,max}^{eb}(j,t) \quad (34)$$
$$u_{char,min}^{ess}(t) < u_{char}^{ess}(t) < u_{char,max}^{ess}(t) \quad (35)$$
$$u_{dis,min}^{ess}(t) < u_{dis}^{ess}(t) < u_{dis,max}^{ess}(t) \quad (36)$$

Besides, charging and discharging states cannot occur simultaneously:

$$u_{char}^{ev}(i,t) * u_{dis}^{ev}(i,t) = 0 \quad (37)$$
$$u_{char}^{eb}(j,t) * u_{dis}^{eb}(j,t) = 0 \quad (38)$$
$$u_{char}^{ess}(t) * u_{dis}^{ess}(t) = 0 \quad (39)$$

And the departure time is always greater than the arrival one:

$$t_{i,d} > t_{i,a} \quad (40)$$
$$t_{j,d} > t_{j,a} \quad (41)$$

V. APPLICATION TO CASE STUDIES

A. SIMULATION SETUP

To demonstrate the effectiveness of the developed algorithm in harnessing the onsite produced and stored energy to supply the peak load, the MPC-based scheduling optimization problem was applied to a real campus integrated microgrid located in Kenitra, Morocco. The microgrid is connected to the DNO and consists of 49.14 kW of photovoltaic parking shades, an ESS of 96 kWh, and a charging station for both EVs and EBs as shown in Fig. 3 [31]. The total number of the available EVs and EBs is 2 and 10, with a maximum storage capacity of 14.5 kWh and 468 Wh respectively. They are considered to be an extent of the energy storage system

FIGURE 3. Kenitra's campus microgrid.

TABLE 1. Information on electric vehicles and bikes.

	Arrival state (kWh)	Desired departure state (kWh)	Arrival time (h)	Departure time (h)
EV 1	4	14	8	17
EV 2	6	14.5	10	18
EB 1	0.14	0.42	8	17
EB 2	0.3	0.43	9	12h30
EB 3	0.39	0.46	10	13
EB 4	0.12	0.40	8	16
EB 5	0.15	0.41	12	15
EB 6	0.38	0.45	11	18
EB 7	0.11	0.3	14	18
EB 8	0.32	0.46	7	13
EB 9	0.2	0.4	8	14
EB 10	0.29	0.38	10	13h30

FIGURE 4. PV production.

providing an additional capacity of 33.68 kWh with the help of V2C and B2C technologies. Their arrival and departure times, as well as their arrival and desired departure states are reported in Table. 1.

The optimization problem is tested through two case studies to illustrate its actual practices and to assess its performance against different weighting factors. The first case study concerns the resolution of the problem with static weighting factors, while for the second, an advanced scheme using dynamic weighting factors is proposed. The mathematical formulation is implemented and solved using Matlab software, where the length of the prediction and control horizon is set at 24 h with a control and prediction interval set equal to 15 min and 10 min respectively.

B. RESULTS AND DISCUSSION

The case studies mentioned above are considered to study two specific cases where the weighting factors are static and dynamic. For both cases, the optimization problem is solved to find the microgrid optimal control using the predicted solar data of a typical day of March 2020. The PV power generated during this simulation day and computed using these data in the equation (7) of the PV model is shown in Fig. 4. It should be noted that this model was validated by comparing the simulated data with those measured over several days. The validation results showed a good agreement of the model output and the experimental data, as depicted in Fig. 5.

1) CASE STUDY 1: STATIC WEIGHTING FACTORS
- Equal weighting factors (EWF) ($\chi = \psi = \theta = \lambda = 1$): In this case, the proposed control strategy has been resolved by giving equal importance to the 4 sub-objective functions.

The results of the peak shaving strategy in the case of EWF are depicted in Fig. 6. As it is well illustrated, the peak load occurs from 8.45 a.m. to 12.15 p.m., where the forecast load exceeds the subscribed power fixed at 100 kW. During this interval of time, the CMS manages the microgrid power flow in a way to fill the power consumption profile while reducing
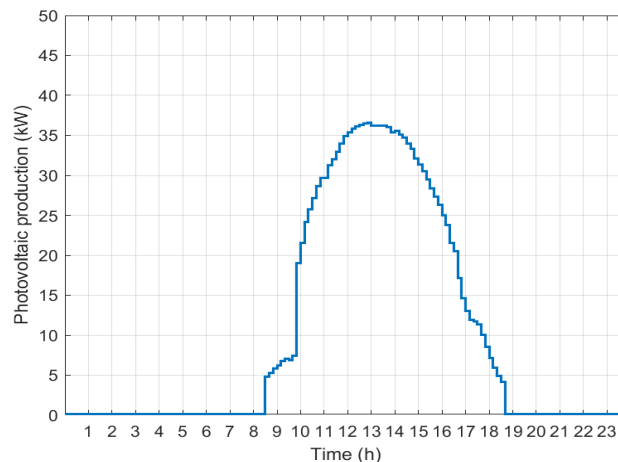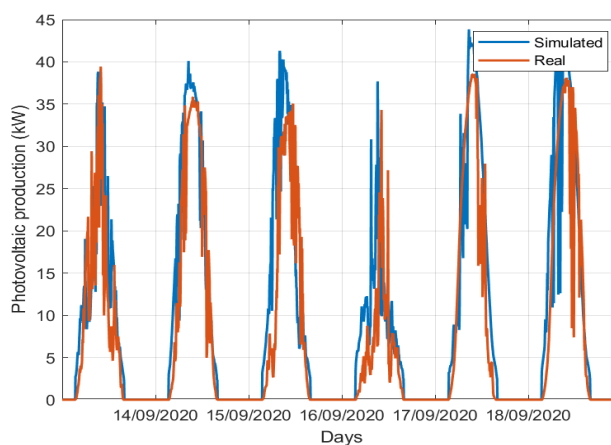
FIGURE 5. Comparison between real and measured PV production.

the energy purchased from the utility grid so as not to exceed the maximum allowable power demand. This is achieved by either harnessing the PV power or discharging the available storage systems (ESS, EVs and EBs), and by drawing the remaining energy from the utility grid. The results show that the power profile is reduced during the peak period by almost 11.95%. The main contributor is the PV production system, followed by EBs and EVs respectively (Table. 2). However, the contribution of the ESS is almost zero, due to the fact that both tracking references (peak load shaving and maximizing the storage energy) have the same priority and present conflicting objectives. In fact, setting equal weighting factors has even allowed to increase the stored energy when the PV power becomes available. Fig. 7 depicts the results of the MPC-based optimal behavior of the microgrid ESS. It can be seen that the stored energy remains equal to its initial value set to 65 kWh from 00 a.m. to 8.15 a.m. and starts to gradually increase with the presence of the PV production until reaching its maximal capacity of 96 kWh. Besides, Fig. 8 shows the optimal energy sold to the DNO as calculated using the MPC strategy. In fact, after meeting the load demand and
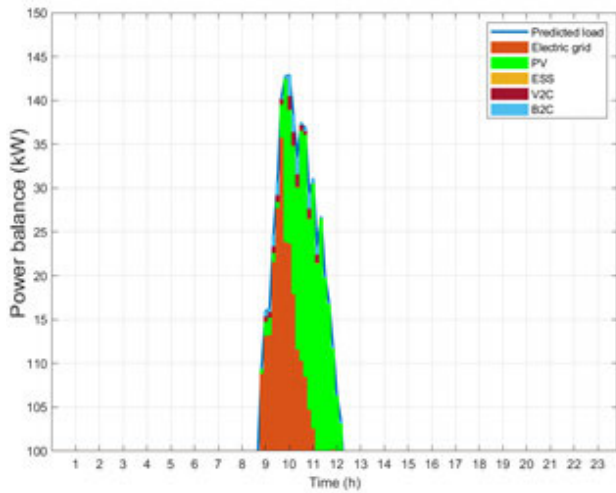
FIGURE 6. MPC-based peak power dispatch in the microgrid in the case of EWF.

TABLE 2. Impact of weighting factors on the grid operation.

	EWF	IWFPESS	IWFPS	DWF
Predicted peak load (kWh)	2638.29	2638.61	2638.71	2639.16
DNO contribution (kWh)	2322.77	2235.33	2232.05	2227.56
PV contribution (kWh)	288.33	344.72	327.43	326.05
ESS contribution (kWh)	0.43	48.14	57.6	65.39
V2C (kWh)	12.62	9.52	13.67	12.8
B2C (kWh)	16.56	14.25	13.36	9.61
Peak reduction (kWh)	315.51	403.28	406.65	411.59
Peak reduction (%)	11.95	15.28	15.41	15.59
Energy sold to DNO (kWh)	1051	999.03	971.27	966.73

FIGURE 7. MPC-based control of the ESS in the case of EWF.
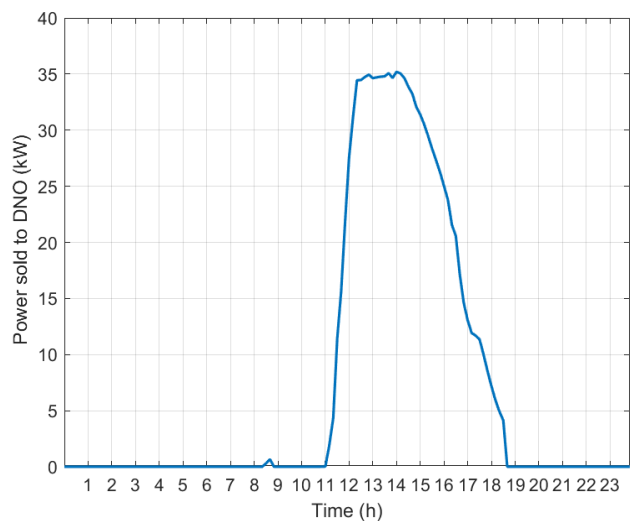
FIGURE 8. Energy sold to DNO in the case of EWF.

satisfying the ESS maximal capacity, the system feeds the utility grid with the excess generated power. In this case, the total energy sold reached a value of 1051 [kWh].

Further, the results show that the peak load was reduced by also exploiting the storage system of the vehicles and bikes available in the campus. Fig. 9 shows the MPC-based control of EVs and EBs in the case of EWF. As it can be seen, the proposed algorithm allowed to deliver a considerable amount of the battery capacity to the microgrid during the peak period while ensuring that the desired state of charge was reached upon departure. More precisely, the EVs and EBs energy balances are reported in Table. 3, where the desired departure state, the MPC-based departure state and the RMSE are detailed. It can be observed that most of the EVs and EBs desired departure states of charge are satisfied with an RMSE of 0.04. A slight deviation was noticed for EB2, EB3 and EB8, since their departure time coincides with the end of the peak load, and their charge rate does not allow to reach the optimal state fast enough.

- Inequal weighting factors (IWFPESS) ($\chi = \psi = \lambda = 1$ and $\theta = 10^{-3}$): In this case, the proposed control strategy has been resolved by penalizing the energy storage system.

The results of the peak shaving strategy in the case of IWF-PESS are depicted in Fig. 10. The figure shows the forecast load curve and the contribution of the microgrid in filling the power consumption profile. It can be seen that the peak load is covered mainly by the PV and ESS thus achieving a peak reduction of 15.28% (Table. 2). This can be explained by the fact that the peak load tracking had a preponderant priority than the ESS reference tracking. Unlike the previous case study, the ESS presents different trends of charge and discharge, as shown in Fig. 11. For example, from 8.00 a.m. to 10.45 a.m., the ESS discharges from 8.00 a.m. to supply the parked EBs and EVs, then charges from 8.15 a.m. due to the availability of the PV energy, and discharges again when the peak occurs at 8.45 a.m. After, from 10.45 a.m.,
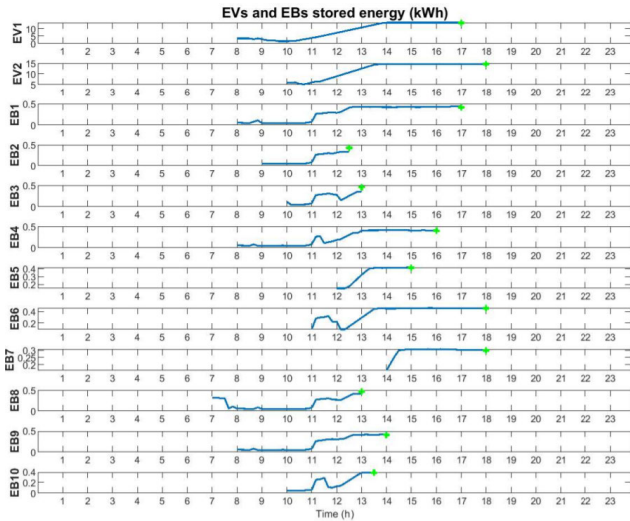
FIGURE 9. MPC-based control of EVs and EBs in the case of EWF.

TABLE 3. Impact of weighting factors on the optimal departure state of EBs and EVs.

	Desired departure state	Optimal departure state			
		EWF	IWFPESS	IWFPS	DWF
EV 1	14	14.01	14.19	11.28	14
EV 2	14.5	14.49	14.48	12.83	14.5
EB 1	0.42	0.43	0.43	0.31	0.42
EB 2	0.43	0.32	0.34	0.07	0.21
EB 3	0.46	0.35	0.34	0.09	0.34
EB 4	0.4	0.40	0.44	0.23	0.33
EB 5	0.41	0.41	0.46	0.11	0.41
EB 6	0.45	0.45	0.37	0.41	0.45
EB 7	0.3	0.30	0.30	0.3	0.29
EB 8	0.46	0.41	0.2	0.11	0.34
EB 9	0.4	0.41	0.4	0.16	0.34
EB 10	0.38	0.38	0.36	0.14	0.32
RMSE		0.04	0.10	0.94	0.08

FIGURE 10. MPC-based peak power dispatch in the microgrid in the case of IWFPESS.
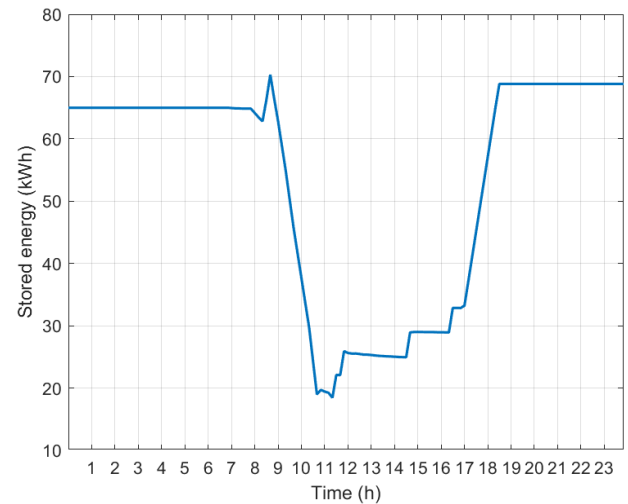
FIGURE 11. MPC-based control of the ESS in the case of IWFPESS.

the battery starts charging gradually taking into account the successive charge and discharge cycles of the available EVs and EBs, until full capacity. Meanwhile, the excess power generated has been fed to the grid as shown in Fig. 12. In fact, setting unequal weighting factors and penalizing the battery tracking allowed the ESS to provide economic benefits by mitigating high-priced electricity consumption at peak times. This strategy also allowed to use the storage system of the EBs and EVs to reduce the peak while satisfying their desired departure states, as shown in Fig. 13.

• Inequal weighting factors (IWFPS) ($\chi = 1$ and $\psi = \lambda = \theta = 10^{-3}$): In this case, the proposed control strategy has been resolved by penalizing the whole storage.

The results of the peak shaving strategy in the case of IWFPS are depicted in Fig. 14. Regarding this shaving case study, the peak reduction rate reached 15.41% due to EBs and EVs additional contributions (Table. 2). In fact, setting high weightage to peak shaving has unfairly disadvantaged

the ESS and EVs/EBs as shown in Fig. 15 and Fig. 17, respectively. First, for ESS, the evolution of the stored energy as computed using the MPC shows a real storage penalty. The latter is perceived when the photovoltaic energy available at 8.15 a.m. has not been stored but rather sold to the DNO as shown in Fig. 15 and Fig. 16. The penalty is also levied when the surplus energy has been sold and not stored until the battery reaches its minimum allowable value from 11.00 a.m. to 01.00 p.m. Then, for EVs and EBs, Fig. 17 and Table. 3 show that the gap between the desired departure state and the optimal departure state has grown, even if the departure time does not conflict with the peak period. Their low weighting factor implied that the energy has been sold instead of having satisfied their desired state of charge.
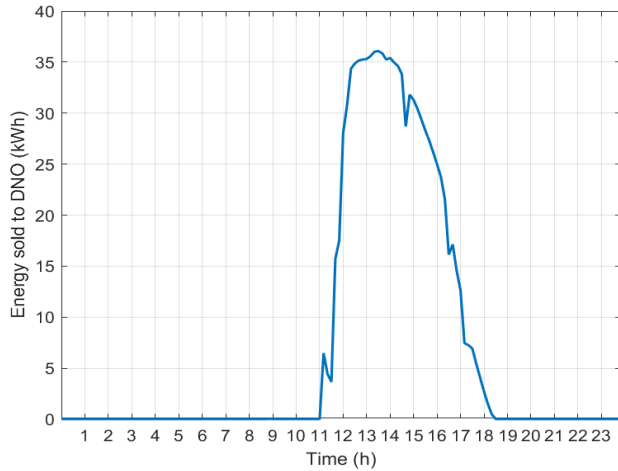
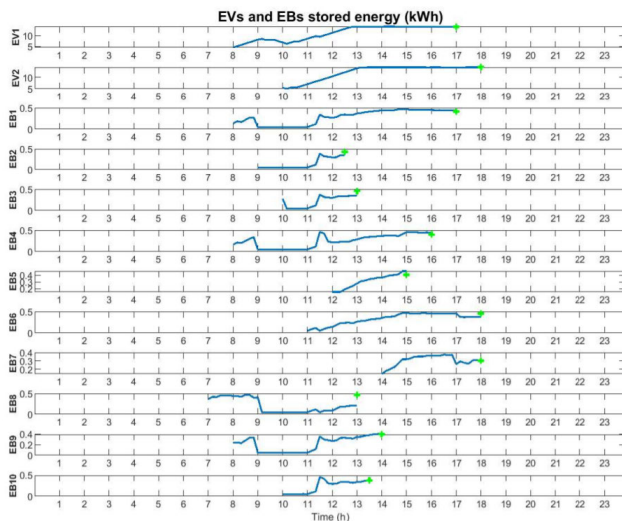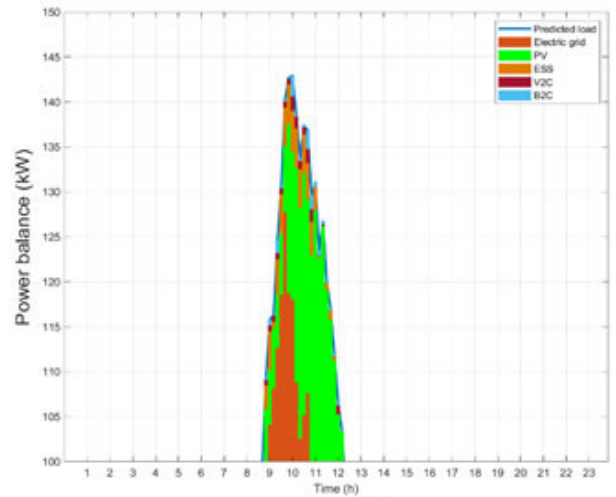**FIGURE 12.** Energy sold to DNO in the case of IWFPESS.

FIGURE 13. MPC-based control of EVs and EBs in the case of IWFPESS.

FIGURE 14. MPC-based peak power dispatch in the microgrid in the case of IWFPS.
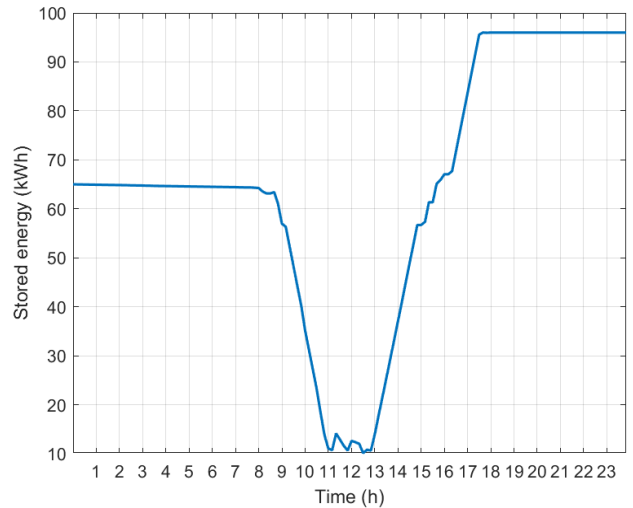
FIGURE 15. MPC-based control of the ESS in the case of IWFPS.

2) CASE STUDY 2: DYNAMIC WEIGHTING FACTORS (DWF)

Instead of using static weighting factors that reduce the system dynamic performance to some extent, the dynamic weighting factors adjustment is proposed in this section. The dynamic weighting factors ensure that all sub-objective functions will be given priority when most needed. They are defined as follows:

- 8h->12h: priority to campus load tracking ($\chi = 1$ *and* $\psi = \lambda = \theta = 10^{-3}$)
- 12h->14h: priority to satisfy EBs state of charge ($\lambda = 1$ *and* $\chi = \psi = \theta = 10^{-3}$)
- 14->16h30: priority to satisfy the ESS state of charge ($\theta = 1$ *and* $\chi = \psi = \lambda = 10^{-3}$)
- 16h30->18h: priority to satisfy EVs state of charge ($\psi = 1$ *and* $\chi = \lambda = \theta = 10^{-3}$)
- 18h->19h: priority to satisfy the ESS state of charge ($\theta = 1$ *and* $\chi = \psi = \lambda = 10^{-3}$)
- otherwise: equal weighting factors

The shaving results in the case of DWF are shown in the following figures. Detailed results of the impacts of the different weighting factors strategies on the campus operation and on the optimal departure state of EBs and EVs are depicted in Table. 2 and 3, respectively. Table. 2 reports the predicted peak load, the contribution of each component of the microgrid, the peak reduction and the amount of energy sold to DNO, while Table. 3 reports the MPC-based optimal departure states of EBs and EVs. As it can be seen, the DWF scenario presents the best performances compared to the previous case studies in term of peak reduction (411.59 kWh ∼ 15.59%) and satisfaction of EVs and EBs desired state (RMSE = 0.08). DWF allows high priority to be given to tracking a sub-objective function when necessary, so that the discharge of ESS, EBs and EVs is promoted to cover the charge deficit during peak periods, the charge of EBs and EVs
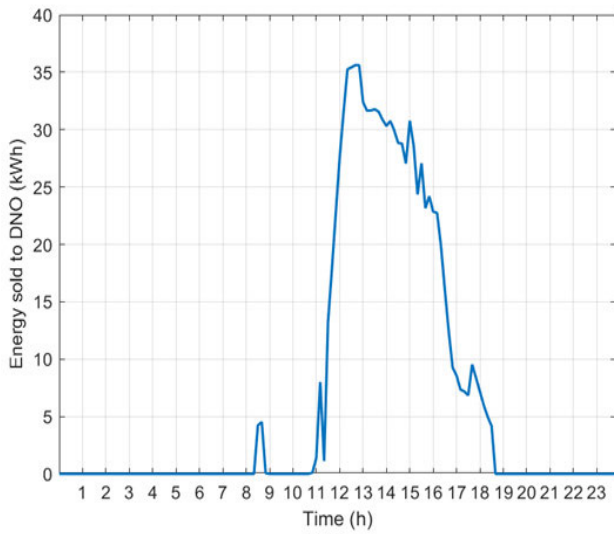
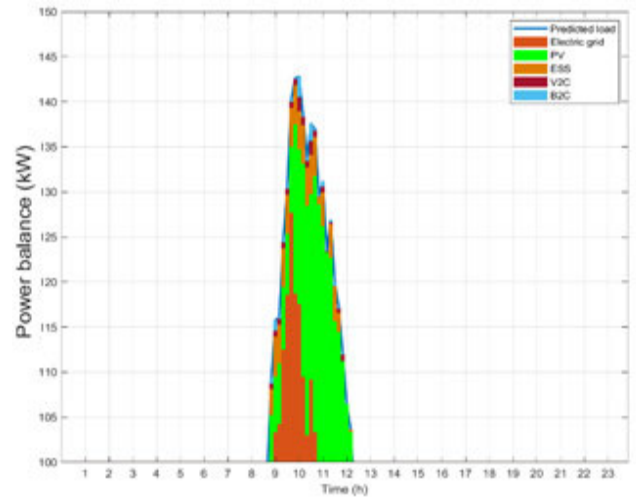**FIGURE 16.** Energy sold to DNO in the case of IWFPS.

FIGURE 18. MPC-based peak power dispatch in the microgrid in the case of DWF.
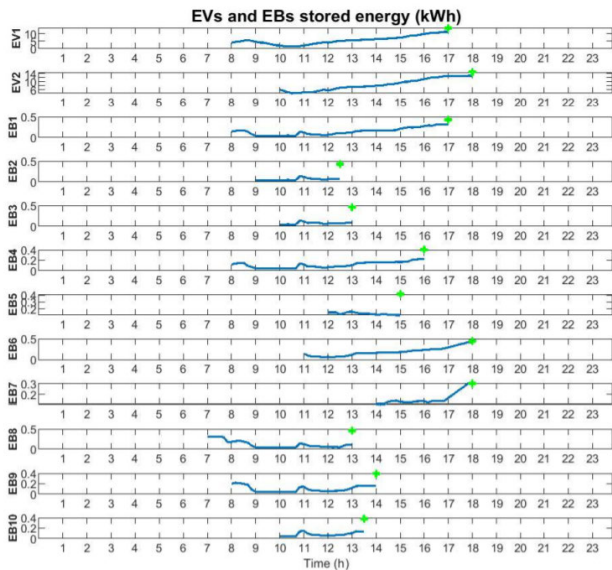

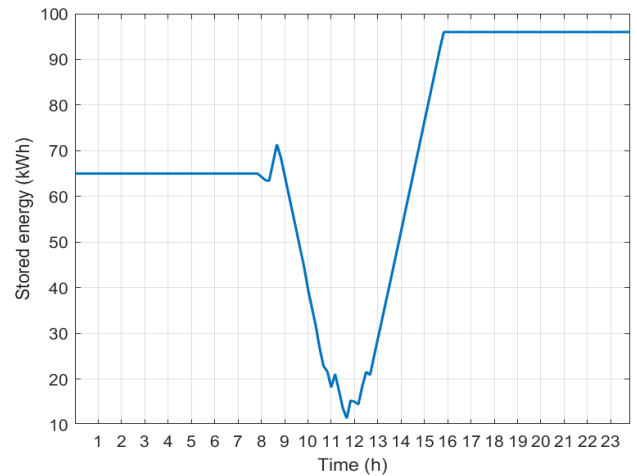**FIGURE 17.** MPC-based control of EVs and EBs in the case of IWFPS.

FIGURE 19. MPC-based control of the ESS in the case of DWF.

is favored just before their departure time, and the charge of the ESS is boosted before proceeding with the sale.

The scheduling optimization problem has been solved considering perfect predictions (deterministic) for the whole horizon. The aim is to assess the influences of forecast errors of the solar irradiation on the optimal operation scheduling of the microgrid. Fig. 21 shows a comparison among the optimal energy sold to the DNO as determined by the MPC strategy and the deterministic method. The analysis of the figure proves that the MPC-based algorithm handles well the stochastic behavior of the inputs and significantly improves the performance of the optimal operation of the microgrid.

The optimization problem has been solved over the whole-time horizon considering that the expected solar production

is determined as the sum of a deterministic part calculated considering measured data and a noise defining the intermittent behavior of the solar irradiation represented by the inverse normal distribution. The aim is to assess the effects of the variabilities of the energy production on the optimal schedule of the microgrid. A comparison among the optimal scheduling of the energy storage state under presence of a noise and as calculated by the receding horizon based MPC scheme is reported in Fig. 22. It can be observed that the energy storage state shows some deviations among the two methods.

Fig. 23 reports the time varying state of the optimal operation of the ESS considering The MPC and Minmax methods. It can be observed the optimal control based MPC provides the ESS with more charging capacities, which enhance the quality of service of the microgrid.
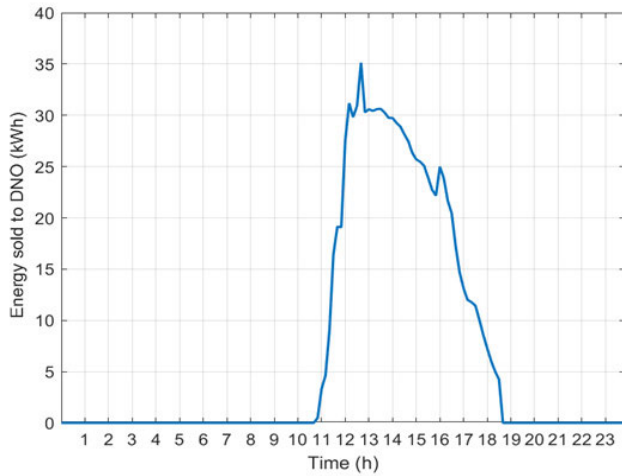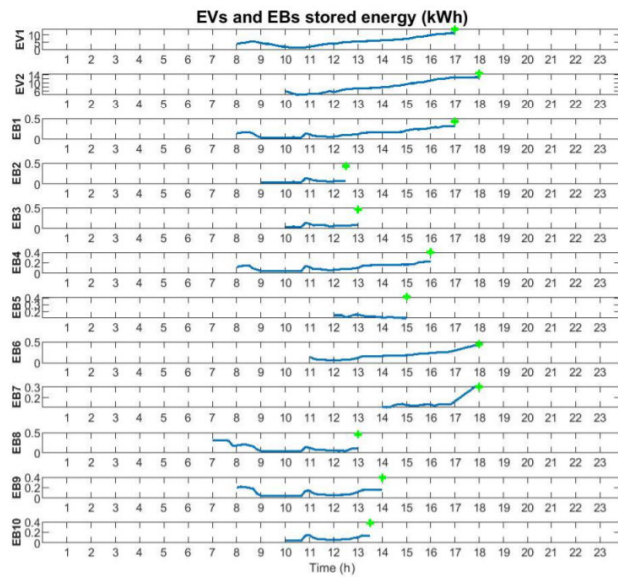
FIGURE 20. Energy sold to DNO in the case of DWF.

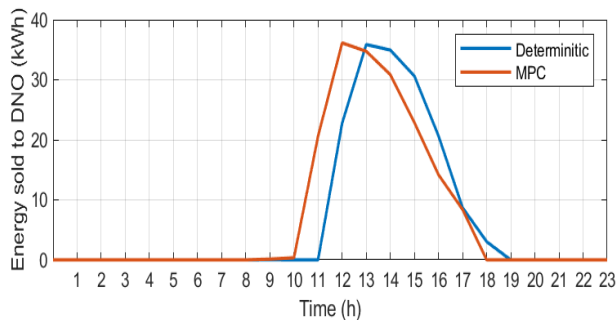**FIGURE 21.** MPC-based control of EVs and EBs in the case of DWF.
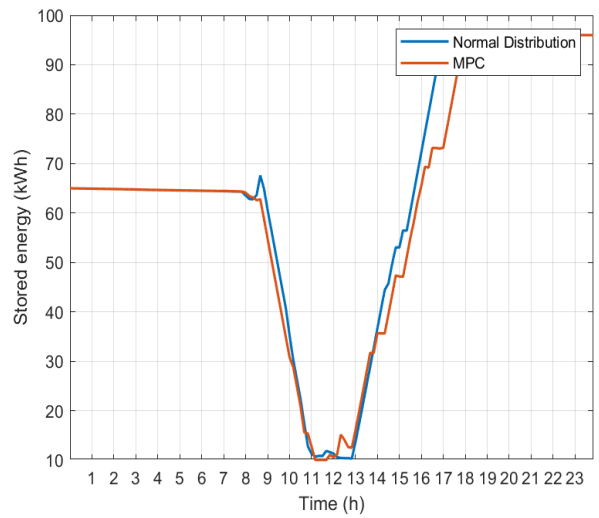

FIGURE 22. Deterministic vs. MPC.

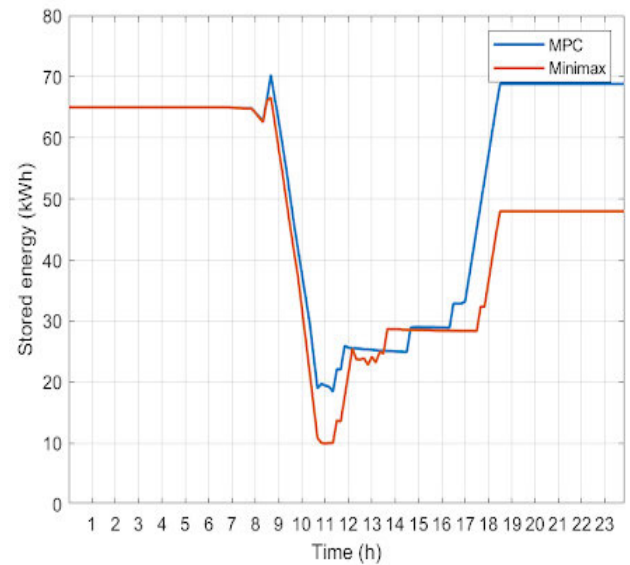**FIGURE 23.** The optimal control of the ESS considering the two approaches.

FIGURE 24. Comparison among MPC and Minmax approaches.

interval, the feedback correction strategy is applied to adjust the control signals of various components of the microgrid.

VI. CONCLUSION

The primary objective of this paper is to illustrate the benefits of model predictive control strategy implementation to an existing campus integrated microgrid with photovoltaic parking shades, electric vehicles and bikes, and an energy storage system, in terms of peak demand reduction. For that, the paper describes this novel and effective MPC-based strategy that aims to exploit the onsite generated and stored energy to supply the exceeding peak. The MPC strategy is formulated to track simultaneously the campus load, the ESS reference and the EBs and EVs desired departure states. It is implemented

The figures demonstrate the choice of adopting the MPC-based algorithm that is applied over the prediction time horizon based on feedback correction. This means that, at each

through two different case scenarios where the weighting factors are static and dynamic. In both cases, the proposed control strategy demonstrated its capability to successfully reduce the peak demand. However, the use of static weighting values leads to a suboptimal accuracy compared to the use of dynamic weighting factors. In DWF, the results illustrated that using energy storage systems with V2C and B2C capabilities and PV generation is able of reducing the peak load under realistic operating conditions by up to 15%.

ACKNOWLEDGMENT

REFERENCES

[1] S. M. S. Danish, M. Ahmadi, M. S. S. Danish, P. Mandal, A. Yona, and T. Senjyu, "A coherent strategy for peak load shaving using energy storage systems," *J. Energy Storage*, vol. 32, Dec. 2020, Art. no. 101823, doi: 10.1016/j.est.2020.101823.

[2] Y. Guo, Q. Zhang, and Z. Wang, "Cooperative peak shaving and voltage regulation in unbalanced distribution feeders," *IEEE Trans. Power Syst.*, vol. 36, no. 6, pp. 5235–5244, Nov. 2021, doi: 10.1109/TPWRS.2021.3069781.

[3] M. Uddin, M. F. Romlie, M. F. Abdullah, S. A. Halim, A. H. A. Bakar, and T. C. Kwang, "A review on peak load shaving strategies," *Renew. Sustain. Energy Rev.*, vol. 82, pp. 3323–3332, Feb. 2018, doi: 10.1016/j.rser.2017.10.056.

[4] M. Kohansal and H. Mohsenian-Rad, "Price-maker economic bidding in two-settlement pool-based markets: The case of time-shiftable loads," *IEEE Trans. Power Syst.*, vol. 31, no. 1, pp. 695–705, Jan. 2016, doi: 10.1109/TPWRS.2015.2405084.

[5] B. N. Silva, M. Khan, and K. Han, "Futuristic sustainable energy management in smart environments: A review of peak load shaving and demand response strategies, challenges, and opportunities," *Sustainability*, vol. 12, no. 14, p. 5561, Jul. 2020, doi: 10.3390/su12145561.

[6] B.-R. Ke, T.-T. Ku, Y.-L. Ke, C.-Y. Chuang, and H.-Z. Chen, "Sizing the battery energy storage system on a university campus with prediction of load and photovoltaic generation," *IEEE Trans. Ind. Appl.*, vol. 52, no. 2, pp. 1136–1147, Mar./Apr. 2016, doi: 10.1109/TIA.2015.2483583.

[7] E. Reihani, M. Motalleb, R. Ghorbani, and L. S. Saoud, "Load peak shaving and power smoothing of a distribution grid with high renewable energy penetration," *Renew. Energy*, vol. 86, pp. 1372–1379, Feb. 2016, doi: 10.1016/j.renene.2015.09.050.

[8] J. S. Hwang, I. Rosyiana Fitri, J.-S. Kim, and H. Song, "Optimal ESS scheduling for peak shaving of building energy using accuracy-enhanced load forecast," *Energies*, vol. 13, no. 21, p. 5633, Oct. 2020, doi: 10.3390/en13215633.

[9] J. P. Fossati, A. Galarza, A. Martín-Villate, and L. Fontán, "A method for optimal sizing energy storage systems for microgrids," *Renew. Energy*, vol. 77, pp. 539–549, May 2015, doi: 10.1016/j.renene.2014.12.039.

[10] C. Lu, H. Xu, X. Pan, and J. Song, "Optimal sizing and control of battery energy storage system for peak load shaving," *Energies*, vol. 7, no. 12, pp. 8396–8410, Dec. 2014, doi: 10.3390/en7128396.

[11] Z. Wang and S. Wang, "Grid power peak shaving and valley filling using vehicle-to-grid systems," *IEEE Trans. Power Del.*, vol. 28, no. 3, pp. 1822–1829, Jul. 2013, doi: 10.1109/TPWRD.2013.2264497.

[12] X. Li, Y. Tan, X. Liu, Q. Liao, B. Sun, G. Cao, C. Li, X. Yang, and Z. Wang, "A cost-benefit analysis of V2G electric vehicles supporting peak shaving in Shanghai," *Electr. Power Syst. Res.*, vol. 179, Feb. 2020, Art. no. 106058, doi: 10.1016/j.epsr.2019.106058.

[13] R. Ghotge, Y. Snow, S. Farahani, Z. Lukszo, and A. van Wijk, "Optimized scheduling of EV charging in solar parking lots for local peak reduction under EV demand uncertainty," *Energies*, vol. 13, no. 5, p. 1275, Mar. 2020, doi: 10.3390/en13051275.

[14] A. F. Meyabadi and M. H. Deihimi, "A review of demand-side management: Reconsidering theoretical framework," *Renew. Sustain. Energy Rev.*, vol. 80, pp. 367–379, Dec. 2017, doi: 10.1016/j.rser.2017.05.207.

[15] H. Hao, C. D. Corbin, K. Kalsi, and R. G. Pratt, "Transactive control of commercial buildings for demand response," *IEEE Trans. Power Syst.*, vol. 32, no. 1, pp. 774–783, Jan. 2017, doi: 10.1109/TPWRS.2016.2559485.

[16] S. L. Arun and M. P. Selvan, "Intelligent residential energy management system for dynamic demand response in smart buildings," *IEEE Syst. J.*, vol. 12, no. 2, pp. 1329–1340, Jun. 2018, doi: 10.1109/JSYST.2017.2647759.

[17] V. S. K. Murthy Balijepalli, V. Pradhan, S. A. Khaparde, and R. M. Shereef, "Review of demand response under smart grid paradigm," in *Proc. ISGT-India*, 2011, pp. 236–243, doi: 10.1109/ISET-India.2011.6145388.

[18] X. H. Li and S. H. Hong, "User-expected price-based demand response algorithm for a home-to-grid system," *Energy*, vol. 64, pp. 437–449, Jan. 2014, doi: 10.1016/j.energy.2013.11.049.

[19] H. Golmohamadi, "Operational scheduling of responsive prosumer farms for day-ahead peak shaving by agricultural demand response aggregators," *Int. J. Energy Res.*, vol. 45, no. 1, pp. 938–960, Jan. 2021, doi: 10.1002/er.6017.

[20] H. Dagdougui, A. Ouammi, and L. A. Dessaint, "Peak load reduction in a smart building integrating microgrid and V2B-based demand response scheme," *IEEE Syst. J.*, vol. 13, no. 3, pp. 3274–3282, Sep. 2019, doi: 10.1109/JSYST.2018.2880864.

[21] A. Ouammi, "Peak loads shaving in a team of cooperating smart buildings powered solar PV-based microgrids," *IEEE Access*, vol. 9, pp. 24629–24636, 2021, doi: 10.1109/ACCESS.2021.3057458.

[22] F. A. Diawuo, M. Sakah, P. C. Baptista, and C. A. Silva, "Assessment of multiple-based demand response actions for peak residential electricity reduction in Ghana," *Sustainable Cities Soc.*, vol. 59, Dec. 2020, Art. no. 102235, doi: 10.1016/j.scs.2020.102235.

[23] D. Dongol, T. Feldmann, and E. Bollin, "A model predictive control based peak shaving application for a grid connected household with photovoltaic and battery storage," in *Proc. 7th Int. Conf. Smart Cities Green Syst.*, Madeira, Portugal, 2018, pp. 54–63, doi: 10.5220/0006685300540063.

[24] D. Dongol, T. Feldmann, M. Schmidt, and E. Bollin, "A model predictive control based peak shaving application of battery for a household with photovoltaic system in a rural distribution grid," *Sustain. Energy, Grids Netw.*, vol. 16, pp. 1–13, Dec. 2018, doi: 10.1016/j.segan.2018.05.001.

[25] D. T. Vedullapalli, R. Hadidi, B. Schroeder, and R. Baumgartner, "Adaptive scheduling of the battery for peak shaving using model predictive control," in *Proc. IEEE Electron. Power Grid (eGrid)*, Charleston, SC, USA, Nov. 2018, pp. 1–5, doi: 10.1109/eGRID.2018.8598693.

[26] X. Guan, Z. Xu, and Q.-S. Jia, "Energy-efficient buildings facilitated by microgrid," *IEEE Trans. Smart Grid*, vol. 1, no. 3, pp. 243–252, Dec. 2010, doi: 10.1109/TSG.2010.2083705.

[27] Y. Achour, A. Ouammi, D. Zejli, and S. Sayadi, "Supervisory model predictive control for optimal operation of a greenhouse indoor environment coping with food-energy-water Nexus," *IEEE Access*, vol. 8, pp. 211562–211575, 2020, doi: 10.1109/ACCESS.2020.3037222.

[28] M. J. Mirzaei, A. Kazemi, and O. Homaee, "A probabilistic approach to determine optimal capacity and location of electric vehicles parking lots in distribution networks," *IEEE Trans. Ind. Informat.*, vol. 12, no. 5, pp. 1963–1972, Oct. 2016, doi: 10.1109/TII.2015.2482919.

[29] A. Ouammi, H. Dagdougui, L. Dessaint, and R. Sacile, "Coordinated model predictive-based power flows control in a cooperative network of smart microgrids," *IEEE Trans. Smart Grid*, vol. 6, no. 5, pp. 2233–2244, Sep. 2015, doi: 10.1109/TSG.2015.2396294.

[30] ONEE. (Jan. 2021). *Site Officiel de ONEE—Branche Electricit*. [Online]. Available: http://www.one.org.ma/FR/pages/interne.asp?esp=1&id1=2&id2=35&id3=119&t2=1&t3=1

[31] *Production Dlectricit Energies Renouvelables*, Univ. Ibn Tofail, Kenitra, Morocco, Nov. 2019. [Online]. Available: https://www.uit.ac.ma/production-delectricite-via-energies-renouvelables/
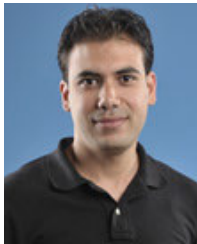
YASMINE ACHOUR received the degree in electrical engineering from the National School of Applied Sciences of Kenitra, Kenitra, Morocco, in 2016. She held the hardware development engineer position with the Research and Development Department of several multinationals operating in the automotive sector, like LEAR Corporation and FAAR Industry. Her current research interests include agricultural greenhouse optimization, renewable energy, efficiency and energy management, and optimization and control of intelligent systems in agriculture.

DRISS ZEJLI was a Researcher with the National Center of Scientific and Technical Research (CNRST-Morocco), Rabat, Morocco, in 1986. He was a Co-Founder of the Unit of Renewable Energy Economy and Technologies (TEER), CNRST, in 1995, and he headed this unit, from 2005 to 2014. In 2014, he joined the National School of Applied Sciences of Kenitra (ENSA-K), Kenitra, Morocco. He is currently a Member Founder of the Desertec University Network (DUN). He has authored and coauthored many papers, conferences, and books on both renewable energies and renewable energy powered desalination. His main research interests include solar and wind energies, renewable energy powered desalination, energy–water–food nexus, and smart agriculture. He was the Chair of the NGO Moroccan Society of Renewable Energy Development (SMADER), from 2013 to 2016.

● ● ●

AHMED OUAMMI received the Ph.D. degree from the Polytechnic School, University of Genoa, Italy, in 2010. He was a Research Fellow with the University of Genoa and worked as an Assistant Professor at the National Centre for Scientific and Technical Research (CNRST). He is currently a Research Associate Professor with Qatar University. His research interests include decision support models, control and optimization of smart grids, and microgrids, with special focus on the implementation of original methods, models, and optimal control algorithms with applications to cooperative and interconnected smart systems integrated renewable energy systems.